



POLITECNICO
MILANO 1863

Orbital Mechanics Project 2022-23

Team n°: **2203**

P. Code	Surname	Name
10882032	Aranda Romero	Fernando
10675538	Arioli	Andrea
10663873	Degener	Martín
10667627	Longari	Riccardo

Course of Orbital Mechanics
Prof: C. Colombo
M.Sc Space Engineering
Academic Year 2022-2023

Contents

1 Assignment 1 - Interplanetary Explorer Mission	3
1.1 Mission goals	3
1.2 Design Approach	3
1.3 Grid Search	4
1.3.1 Coarse Grid search	4
1.3.2 Refined Grid search	5
1.3.3 Gradient based optimization	6
1.4 Minimal Cost Solution	6
1.4.1 Heliocentric Trajectory	6
1.4.2 Flyby	7
1.4.3 Total Cost	7
2 Assignment 2 - Planetary Explorer Mission	8
2.1 Mission goals	8
2.2 Perturbations	8
2.2.1 J_2 perturbation	8
2.2.2 Moon perturbation	8
2.3 Ground tracks	8
2.4 Propagation of the orbit	10
2.5 Evolution of the orbit	12
2.6 Comparison with real data	13

List of Figures

1.1 Porkchop Plot for Earth Saturn trajectory	5
1.2 SC pointing performance - control enabled	5
1.3 First 100 minima for Earth-Saturn-NEO90 (Refined)	6
1.4 Heliocentric Trajectory.	7
1.5 Flyby in Saturn's Perifocal Frame.	7
1.6 Saturn's SOI in Saturn's Perifocal Frame.	7
2.1 Ground track over 1 period	9
2.2 Ground track over 1 day	9
2.3 Ground track over 10 days	9
2.4 Comparison between Starting and Ending points	10
2.5 Evolution of keplerian elements over 100 orbits	10
2.6 Evolution of keplerian elements over 10 orbits	11
2.7 Compare: Gaussian with only J_2 perturbation and Cartesian with both J_2 and lunar perturbations	11
2.8 Differences in keplerian parameters between Gaussian and Cartesian approaches	12
2.9 Propagation over 1000 orbits	12
2.10 Comparison of keplerian elements with ephemerides over 1 year	13
2.11 Difference between ephemerides and propagation from initial parameters	13

List of Tables

1.1 Interplanetary Explorer Mission Specifications.	3
1.2 Minimal Cost Mission.	6
1.3 Transfer Arcs Characterization.	6
1.4 Flyby Characterization.	7
1.5 Detailed Mission Cost.	7
2.1 Initial Orbital Parameters	8

2.2	Computational time comparison	12
2.3	Initial Orbital Parameters of the Debris	13

List of Symbols

Variable	Description	Unit	Variable	Description	Unit
a	Semi-Major Axis	km	T	Orbital Period	s
e	Eccentricity	-	T_e	Earth Rotation Period	s
Δv	Manoeuvre Cost	km/s	T_{rep}	Orbital Period of Repeating Ground Track Orbit	s
Δ	Impact Parameter	km	a_{rep}	Semi-Major Axis of Repeating Ground Track Orbit	s
δ	Flyby Turning Angle	deg	J_2	Gravitational Field Constant of the Earth	-
$\Delta\theta$	Transfer Angle	deg	μ	Earth Planetary Constant	km ³ /s ²
i	Inclination of the Orbit	rad	μ_{Moon}	Moon Planetary Constant	km ³ /s ²
Ω	Right Ascension of the Ascending Node	rad	R_e	Earth Radius	km
ω	Anomaly of Pericentre	rad	a_{Moon}	Moon Perturbing Acceleration	km/s ²
θ	True Anomaly	rad	$\ddot{\mathbf{r}}_{J_2}$	J_2 Perturbing Acceleration	km/s ²
M_0	Mean Anomaly	rad			
$\mathbf{r}_{SC-3body}$	Spacecraft-Moon Position Vector	km			
$\mathbf{r}_{Earth-3body}$	Earth-Moon Position Vector	km			
$\hat{\mathbf{r}}$	Radial RSW RF Unit Vector	-			
$\hat{\mathbf{s}}$	Along-Track RSW RF Unit Vector	-			
$\hat{\mathbf{w}}$	Cross-Track RSW RF Unit Vector	-			

Acronyms

-	Description
RAAN	Right Ascension of the Ascending Node
ToF	Time of Flight
ode	Ordinary Differential Equation

-	Description
SOI	Sphere Of Influence
RGTR	Repeating Ground Track Ratio

Chapter 1

Assignment 1 - Interplanetary Explorer Mission

1.1 Mission goals

The PoliMi Space Agency has been entrusted with the task of designing an optimal Interplanetary Explorer Mission involving three bodies of the Solar System: Earth, Saturn and NEO90. This project is based on a preliminary analysis of the interplanetary mission using the Patched Conics Method. This analysis studies the first transfer orbit between Earth and Saturn, the powered gravity assist fly-by at Saturn and, finally, the last transfer orbit involving Saturn and NEO90. The mission specifications can be seen in Table 1.1

Departure Planet	Earth
Flyby Planet	Saturn
Arrival NEO	90
Earliest Departure	30-08-28
Latest Arrival	26-02-63

Table 1.1: Interplanetary Explorer Mission Specifications.

1.2 Design Approach

The design approach is based on the Patched Conics Method. The approach divides the mission in two different heliocentric arcs: a first one going from Earth to Saturn and a second one from Saturn to NEO90. To go from one transfer to the other a powered gravity assisted flyby is performed at Saturn. The following considerations are taken into account [1]:

- Planetary departure and insertion are not considered. The initial heliocentric orbit is equal to Earth's orbit and the final heliocentric one is equal to NEO's 90 orbit.
- The spacecraft is considered to begin the heliocentric transfer once it escapes the Sphere Of Influence (SOI) of the planet and the Sun becomes the main body.
- The transfers are solved and the incoming and outgoing boundaries of the Saturn flyby are characterized using a Lambert solver
- From a heliocentric perspective the flyby happens instantaneously.

The minimum cost of the interplanetary mission is found using a 3D mesh iteratively refined. The grid is composed of three different parameters: departure date, time of flight for the first transfer and date of arrival. Finally, the *fminunc* algorithm is used. The following physical constraints are applied to reduce the computational cost [1]:

- The Time of Flight (ToF) of a transfer must be greater than its respective parabolic time, the minimum time to achieve an elliptical trajectory. For lower times, an hyperbolic trajectory is obtained which implies a Δv too high for the main purpose of minimizing the cost.

$$ToF > T_{parabolic}$$

- The ToF of each transfer must be lower than the corresponding time of a Hohmann transfer in each leg. The Hohmann transfer is considered the smoother one and, therefore, the one that has the greatest time.

$$ToF < T_{Hohmann}$$

- The radius at pericentre of the flyby must be greater than the critical radius of Saturn. The critical radius is defined by the radius in which the atmosphere has a pressure equivalent to 1 bar. In this case, the critical radius for Saturn is 60268 km [2].

$$r_{\text{pericentre}} > r_{\text{critical}}$$

- The Δv of each transfer must be less than a threshold value which varies with every refinement.

$$\Delta v < \Delta v_{\text{limit}}$$

1.3 Grid Search

The grid search is performed using the following algorithm. The parallel computing toolbox is used to decrease the computational time. If statements use a positive short circuit thus the loop only runs for points that meet the specified conditions.

Algorithm 1 Interplanetary transfer

Require: Time arrays for Earth departure, time of flight to Saturn and date of arrival to NEO90. ID of planets, gravitational constants of Sun and Saturn, Critical Radius of Saturn, Hohmann transfer time for Earth-Saturn

```

1: for Departure date from Earth do
2:   for Time of Flight to Saturn do
3:     if Time of Flight to Saturn < Time of Hohmann transfer then
4:       Calculate Earth-Saturn transfer. Store results
5:     end if
6:     for Arrival date to NEO90 do
7:       if delta V Earth-Saturn < threshold and Departure date plus time of flight to Saturn < Date of
   Arrival and Time of flight to Saturn > Parabolic transfer time then
8:         Characterize Saturn-NEO90 transfer. Store values
9:       end if
10:      if delta V Saturn-NEO 90 < threshold and Time of flight to NEO90 > Parabolic transfer time
    then
11:        Characterize flyby. Store values
12:      end if
13:      if Radidus at perigee > Critical radius at perigee then
14:        Calculate total delta V cost. Store values
15:      end if
16:    end for
17:  end for
```

1.3.1 Coarse Grid search

The first grid consists of a coarse cutting of the time frame. The departure array is created by selecting a date for every 35 degrees of change in the true anomaly of the Earth. Similarly, the time of flight to the Flyby array is created for every 5 degrees of Saturn, and the arrival array is created for every 30 degrees of NEO90. This returns an initial grid search of 363 by 86 by 166 possible data points. With the conditions described in the design approach, the total computed points for the coarse search are reduced to 108908, or about 2 percent of the array.

Earth-Saturn Transfer

The synodic period between the two planets (378 days) is calculated using the formula

$$T_{\text{syn}} = \frac{1}{\frac{1}{T_{\text{Earth}}} - \frac{1}{T_{\text{Saturn}}}}$$

The coarse search data for the Earth Saturn transfer is used to plot the following porkchop plot

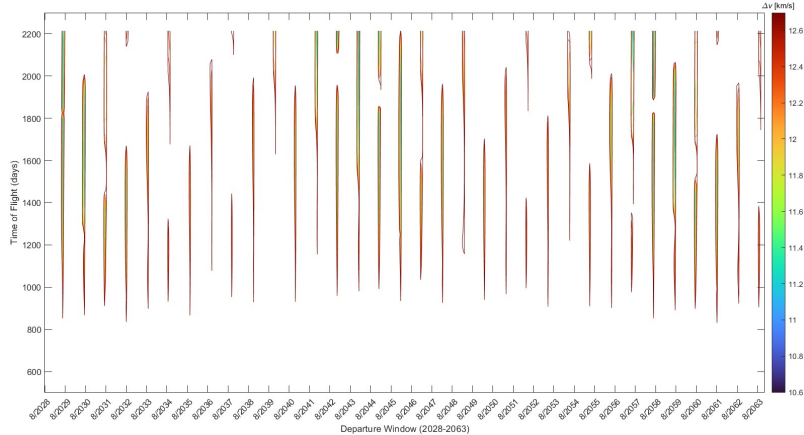


Figure 1.1: Porkchop Plot for Earth Saturn trajectory

In it we can clearly identify the synodic repetition for the minimum cost. Because the synodic period is close to that of Earth's, the ideal transfer time between Earth and Saturn happens somewhere around August with a value between 10 and 11.5 km/s

Minima identification

The first 1000 minima for the entire mission resulting from the coarse search are plotted in figure 1.2b We can appreciate two minima regions, with departure dates grouped around the month of August. Narrowing the minima down to 500, we obtain figure 1.2a

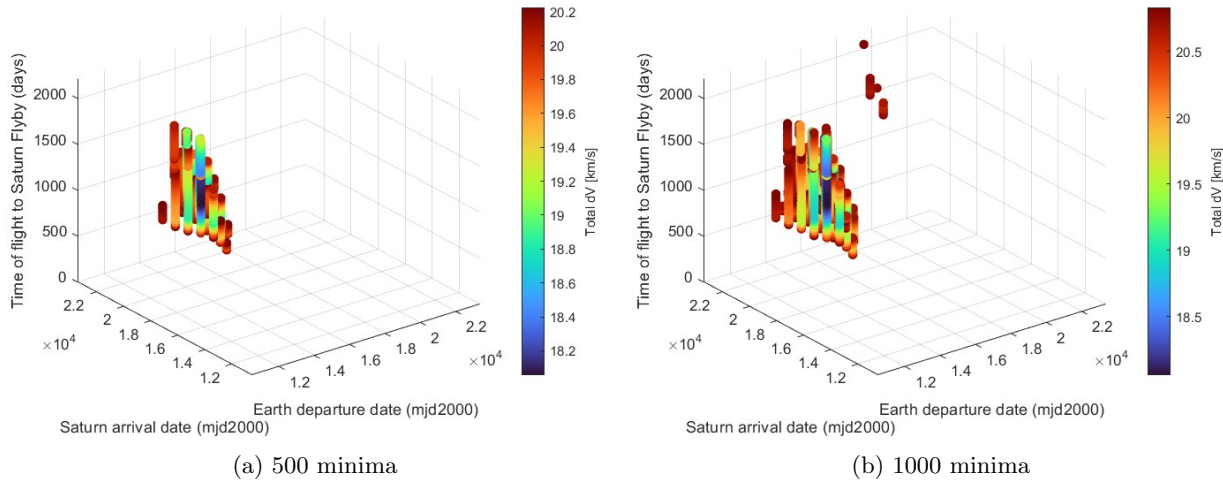


Figure 1.2: SC pointing performance - control enabled

The initial coarse search already allows us to identify the region where the ideal solution will be located. The search area is then reduced to the boundaries of the region defined by this 500 minima.

1.3.2 Refined Grid search

The refined grid is restricted to the ideal area identified during the coarse search. The amount of orbital periods completed by each body during this timeframe is computed and the new time arrays are filled with a point for every 5 degree change in true anomaly. This returns a refined grid of 302 by 8 by 290 datapoints. The refined cost plot is then obtained figure 1.3

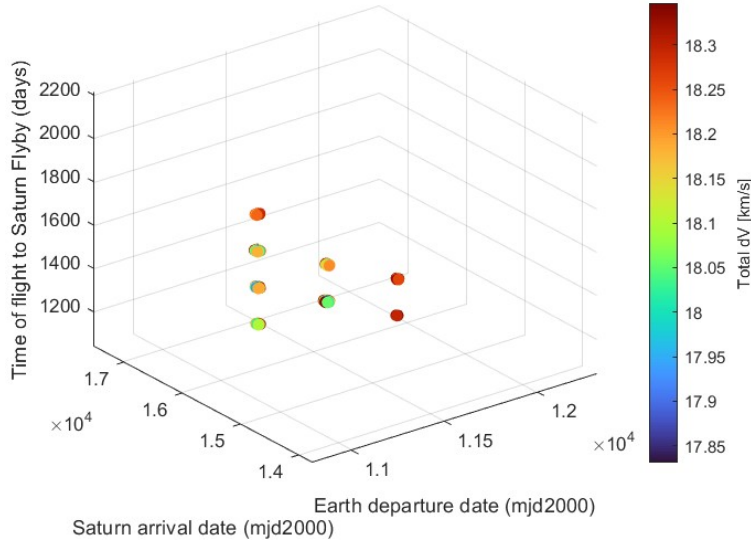


Figure 1.3: First 100 minima for Earth-Saturn-NEO90 (Refined)

1.3.3 Gradient based optimization

A gradient based minimization using MATLAB's *fminunc* is employed to find refine the search one last time. Using the minimum obtained from the refined search as a starting point the final ideal total cost is obtained. The results are discussed in the following section.

1.4 Minimal Cost Solution

The minimal cost interplanetary mission obtained is characterized by the following times and cost displayed in Table 1.2.

Method	Departure Date	Flyby Date	Arrival Date	$\Delta v [km/s]$
Grid Search	2030 Aug 02, 18:29:50	2034 Oct 25, 01:14:27	2040 Apr 28, 00:18:18	17.831
<i>fminunc</i>	2030 Aug 03, 11:46:28	2035 Jan 04, 00:58:16	2040 Apr 26, 06:23:21	17.667

Table 1.2: Minimal Cost Mission.

As it can be seen, both minimums are really close to each other, however, the one found using *fminunc* is more refined.

1.4.1 Heliocentric Trajectory

As it has been said previously, the heliocentric trajectory is characterized by two different transfers, from Earth to Saturn and, then, from Saturn to NEO90. The parameters of each transfer are shown in the Table 1.3

Arc	ToF [days]	a [AU]	e [-]	i [deg]	Ω [deg]	ω [deg]	θ_0 [deg]	$\Delta\theta$ [deg]
Earth - Saturn	1614.5499	5.2920	0.8083	1.8086	5.4316	359.1838	0.8162	170.0024
Saturn - NEO90	1939.2258	5.0007	0.8283	7.8363	5.2970	354.6042	183.0927	275.7887

Table 1.3: Transfer Arcs Characterization.

Both arcs are quite similar in terms of semi-major axis and eccentricity due to the fact that the Earth and NEO90 orbits are quite similar to each other. The biggest difference remains in transfer angle which derives in the longest time of flight for the second arc as the spacecraft must travel a longer distance. Figure 1.4

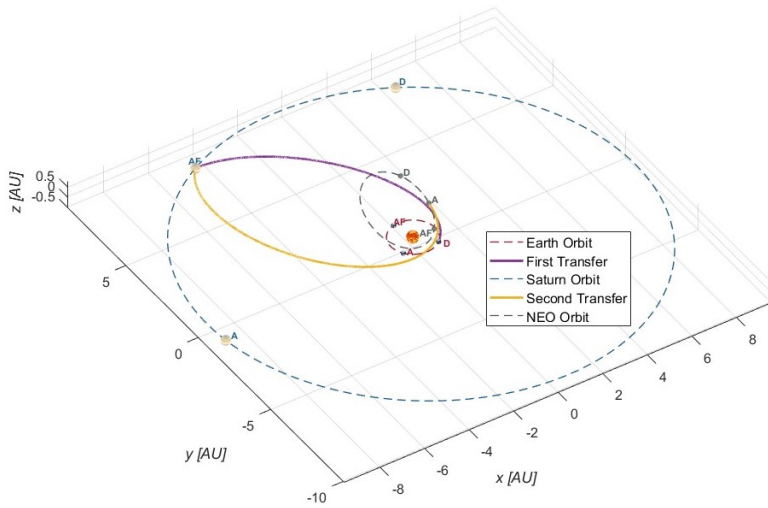


Figure 1.4: Heliocentric Trajectory.

1.4.2 Flyby

In order to characterize the flyby, the incoming and outgoing velocities which are provided by applying the Lambert problem to the transfer arcs must be given.

Figures 1.5 and 1.6 show the flyby performed in Saturn in perifocal frame along with the SOI of the planet. As it can be seen, the sphere of influence is quite large, something that makes sense when the focus is put in the Equation 1.4.2 where $r_{Saturn2Sun}$ is the norm of the distance between Saturn and the Sun. As Saturn is quite far from the Sun and it is one of the biggest planets in the Solar System, its SOI is really significant.

$$SOI_{Saturn} = r_{Saturn2Sun} \frac{\mu_{Saturn}}{\mu_{Sun}}^{2/5} \quad (1.1)$$

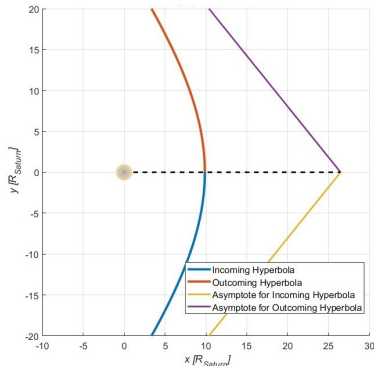


Figure 1.5: Flyby in Saturn's Perifocal Frame.

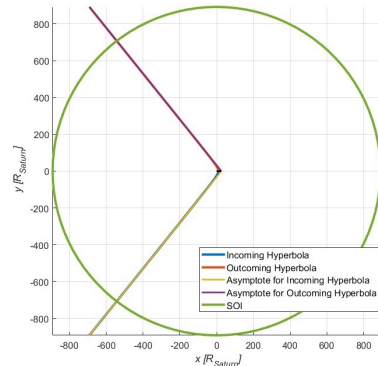


Figure 1.6: Saturn's SOI in Saturn's Perifocal Frame.

Δ_{inc} [km]	Δ_{out} [km]	δ [deg]	r_{peri} [R_{Saturn}]	t_{Flyby} [days]	Δv_{peri} [km/s]	Δv_{Flyby} [km/s]
1200953.6358	1200953.7146	77.6925	9.8709	180.3140	$2.55 \cdot 10^{-7}$	3.938

Table 1.4: Flyby Characterization.

The parameters referring to both hyperbolas of the flyby are displayed in Table 1.4. The secret behind this interplanetary mission remains in the fact that the cost of the powered assist flyby is negligible, significantly reducing the total cost. Because of this, the incoming and outgoing hyperbolas are almost identical. Finally, the time spent performing the flyby is significant as well, as it has been shown, Saturn's SOI is quite large which derives in a big time of flyby.

1.4.3 Total Cost

Δv_{Dep} [km]	Δv_{Flyby} [km]	Δv_{Arr} [km]	Δv_{TOTAL} [km]
10.478	$2.55 \cdot 10^{-7}$	7.189	17.667

Table 1.5: Detailed Mission Cost.

Chapter 2

Assignment 2 - Planetary Explorer Mission

2.1 Mission goals

The goal is to carry out the orbit analysis of a satellite orbiting around Earth, computing the ground track of the orbit itself. To perform the analysis different propagation methods has been used to compute the trajectory of the satellite. In the end, the model has been validated with a comparison with actual ephemerides data of a real debris.

$a[\text{km}]$	$e[-]$	$i[\text{deg}]$	$\Omega[\text{deg}]$	$\omega[\text{deg}]$	$\theta[\text{deg}]$	$T[\text{s}]$	$RGTR$
$2.6566 \cdot 10^4$	0.6369	17.8904	0	0	0	$4.8322 \cdot 10^4$	2 : 1

Table 2.1: Initial Orbital Parameters

2.2 Perturbations

For this analysis have been taken into account the following types of perturbations:

2.2.1 J_2 perturbation

Caused by the oblateness of the Earth, J_2 perturbation bends the direction of the acceleration with the effect that it becomes not exactly parallel to the radial direction. The acceleration components of J_2 can be computed as follows:

$$\ddot{\mathbf{r}}_{J_2} = \frac{3}{2} \frac{J_2 \mu R_e^2}{r^4} \left[\frac{x}{r} \left(5 \frac{z^2}{r^2} - 1 \right) \mathbf{i} + \frac{y}{r} \left(5 \frac{z^2}{r^2} - 1 \right) \mathbf{j} + \frac{z}{r} \left(5 \frac{z^2}{r^2} - 3 \right) \mathbf{k} \right] \quad (2.1)$$

where \mathbf{r} is the position vector of the s/c and x, y, z its Cartesian components.

2.2.2 Moon perturbation

A three-body problem perturbation has been implemented considering the influence of the Moon's gravity field. The perturbing acceleration is therefore computed as follows:

$$\mathbf{a}_{\text{Moon}} = \mu_{\text{Moon}} \left(\frac{\mathbf{r}_{SC-3body}}{r_{SC-3body}^3} - \frac{\mathbf{r}_{Earth-3body}}{r_{Earth-3body}^3} \right) \quad (2.2)$$

The resulting equations of motion in the Cartesian Reference Frame will be therefore:

$$\frac{d^2 \mathbf{r}}{dt^2} = -\frac{\mu}{r^3} \mathbf{r} + \sum \mathbf{a}_p \quad (2.3)$$

Where \mathbf{a}_p are the different perturbing accelerations.

2.3 Ground tracks

First of all, the semi-major axis has been adjusted in order to have a repeating ground track, using the following formulas has been computed the new orbital period and the repeating semi-major axis:

$$T_{rep} = T_e / RGTR = 4.3082 \cdot 10^4 \text{s} \quad a_{rep} = \sqrt[3]{\mu \cdot \left(\frac{T_{rep}}{2\pi} \right)^2} = 2.6562 \cdot 10^4 \text{km} \quad (2.4)$$

The projection of the orbit has been plotted for three different time spans: 1 period, 1 day and 10 days in both cases, with and without perturbations.

Since the $RGTR$ is set to 2:1, the expectations are that the ground track will end up in the same point after two orbits of the s/c.

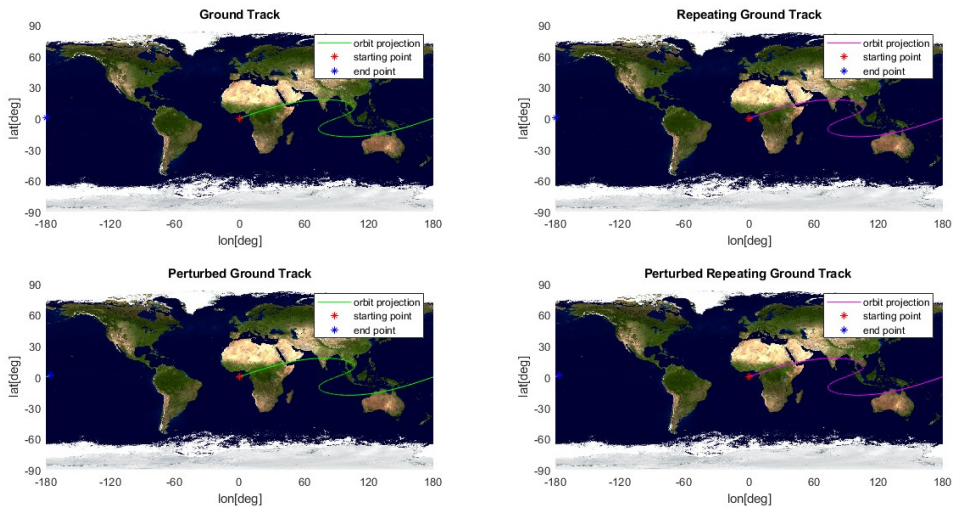


Figure 2.1: Ground track over 1 period

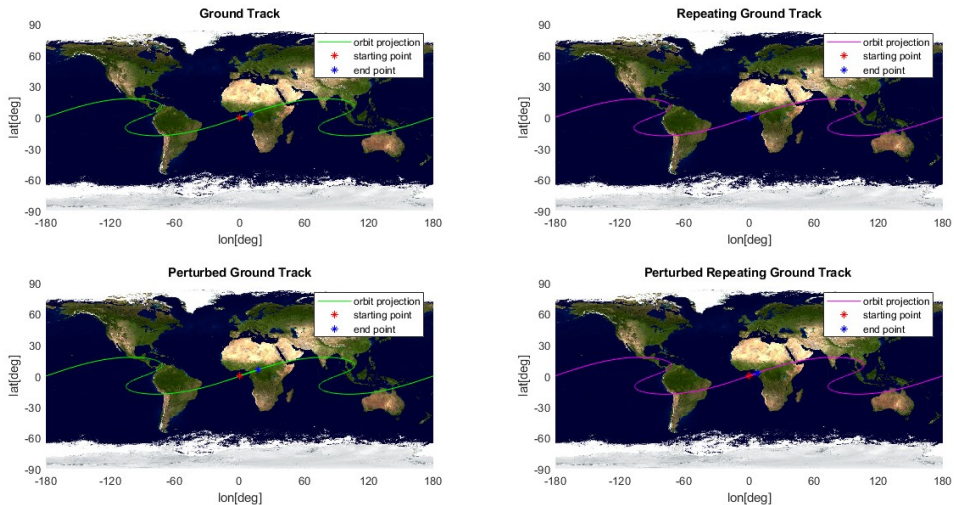


Figure 2.2: Ground track over 1 day

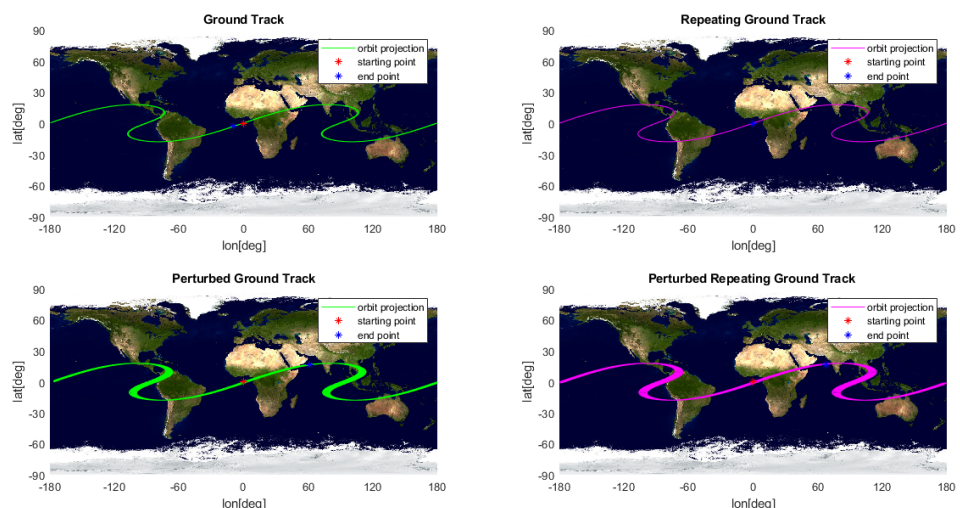


Figure 2.3: Ground track over 10 days

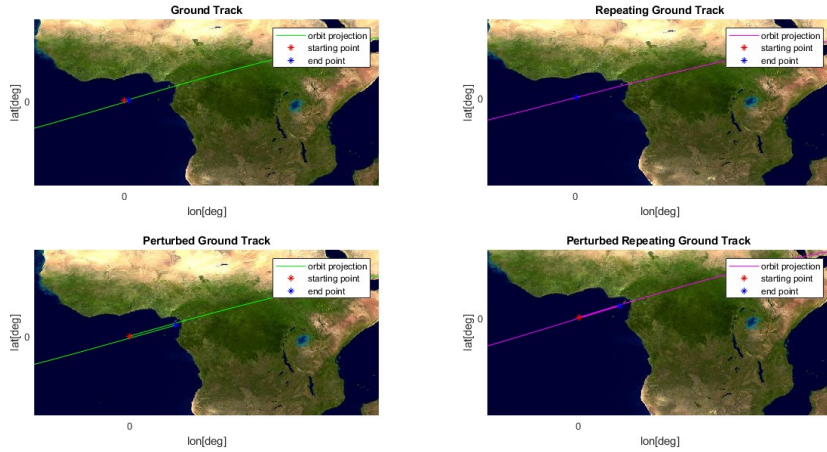


Figure 2.4: Comparison between Starting and Ending points

As expected, the ground track exactly repeats itself only when the perturbing effects aren't taken into account. In fact, there is a shift between two consecutive orbits even with the semi-major axis a_{rep} computed as shown in equation 2.4. This occurs because the perturbing acceleration is responsible for a periodical change in the semi-major axis, which can't be considered when a_{rep} is computed.

All the next steps in the analysis are made considering the initial semi-major axis, not the one computed for the repeating ground track (a_{rep}).

2.4 Propagation of the orbit

To compute the ground tracks under the effect of the perturbations is mandatory to integrate numerically the equations of motion. So Gauss' planetary equations have been integrated, considering the RSW Reference Frame, defined as follows:

$$\hat{\mathbf{r}} = \frac{\mathbf{r}}{r} \quad \hat{\mathbf{w}} = \frac{\mathbf{r} \times \mathbf{v}}{||\mathbf{r} \times \mathbf{v}||} \quad \hat{\mathbf{s}} = \hat{\mathbf{w}} \times \hat{\mathbf{r}} \quad (2.5)$$

To validate the results has been implemented a different numerical model, this time integrating Cartesian equations through an *ode* solver, to compare the outcomes. In order to appreciate the secular evolution of the orbit has also been implemented a low-pass filter, which removes the higher frequency behaviours.

Another type of check can be used since, when is considered only the J_2 effect it is possible to compute analytically the theoretical slope of the RAAN, the anomaly of the pericenter and the mean anomaly as follows:

$$\begin{aligned} \dot{\Omega} &= - \left[\frac{3}{2} \frac{\sqrt{\mu} J_2 R_e^2}{(1-e^2)^2 a^{7/2}} \right] \cos i \quad \dot{\omega} = - \left[\frac{3}{2} \frac{\sqrt{\mu} J_2 R_e^2}{(1-e^2)^{3/2} a^{7/2}} \right] \left(\frac{5}{2} (\sin i)^2 - 2 \right) \\ \dot{M}_0 &= - \left[\frac{3}{2} \frac{\sqrt{\mu} J_2 R_e^2}{(1-e^2)^{3/2} a^{7/2}} \right] \left(1 - \frac{3}{2} (\sin i)^2 \right) \end{aligned}$$

The following results are obtained:

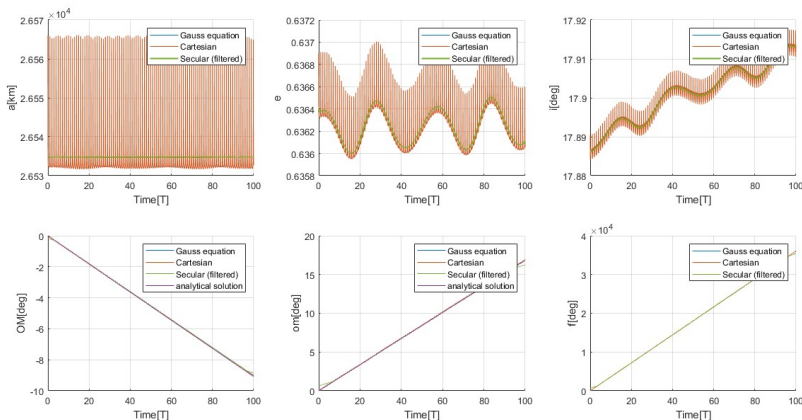


Figure 2.5: Evolution of keplerian elements over 100 orbits

From the analysis of the previous figures, it is possible to notice that the J_2 perturbation acts with a significantly higher frequency with respect to the Moon effect. Moreover it is highlighted the fact that the frequency of the perturbation is linked with the Moon orbital period of 27 days.

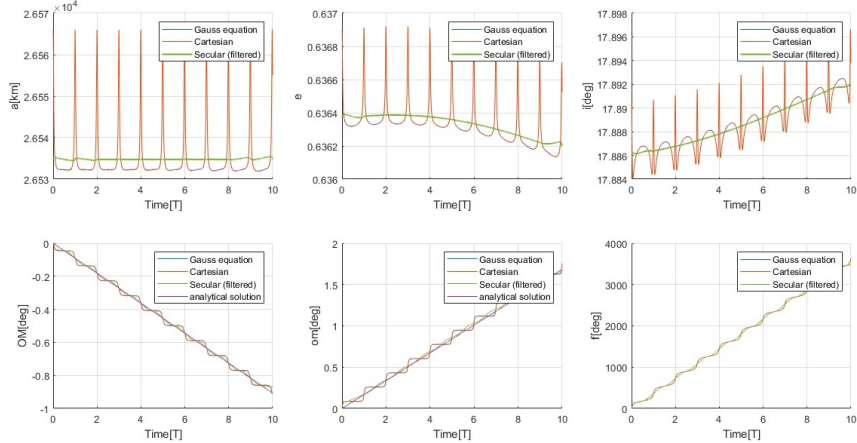


Figure 2.6: Evolution of keplerian elements over 10 orbits

From the previous figure, it is also possible to detect the well-known Gibbs phenomenon, which consists in a less-precise estimate of the function at the border of the domain. To better appreciate the different effects of the two types of perturbations, another orbit has been propagated, this time considering only the effect of the J_2 effect for the Gaussian approach, while keeping both the accelerations in the Cartesian model. This was the result:

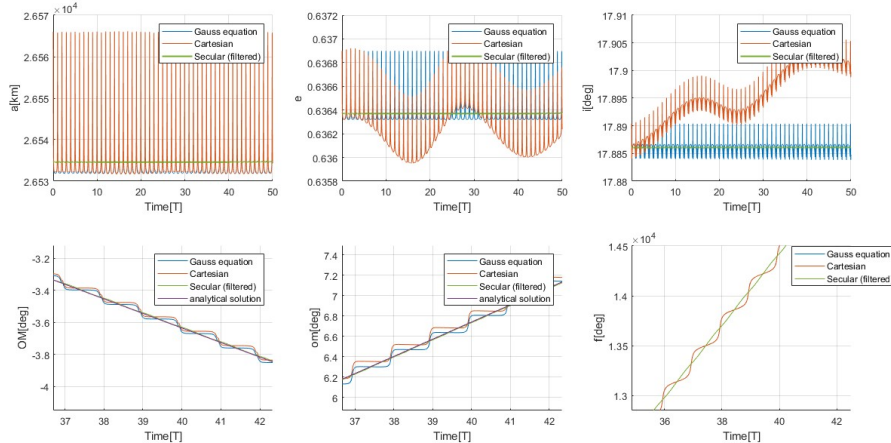


Figure 2.7: Compare: Gaussian with only J_2 perturbation and Cartesian with both J_2 and lunar perturbations

Notice how the secular effect of the Moon perturbation is far more evident on the eccentricity and the inclination of the orbital plane. Also anomaly of the pericentre is affected in a significant way. The difference between Cartesian and Gaussian-based propagation methods considering all the perturbations is shown below:

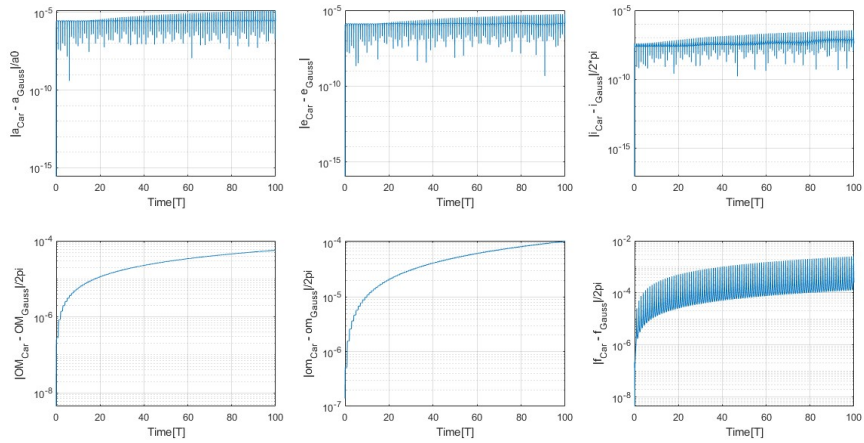


Figure 2.8: Differences in keplerian parameters between Gaussian and Cartesian approaches

It can be noticed that the difference in the results between the two numerical methods seems to be negligible. They are, however, different in terms of computational efficiency, with the Gaussian approach being slightly faster. As example, considering two strategies needed the following amounts of time to perform the integration, for a vector of times with 10^4 elements:

Computational Time [s]		
Method	100 orbits	1000 orbits
Gauss' equations	2.57	34.47
Cartesian equations	3.40	38.65

Table 2.2: Computational time comparison

Some final considerations can be done after the analysis of 2.5 and 2.6 figures:

- The semi-major axis is affected by high frequency perturbation, while, in the long period, it varies only slightly because Moon perturbation does not substantially influence it.
- Eccentricity and inclination, on the other hand, change visibly in their secular behaviour, but they present relatively low oscillation in magnitude.
- The *RAAN*, the anomaly of the pericentre and the true anomaly present a secular linear evolution.

2.5 Evolution of the orbit

Using the numerical propagator of the orbit based on the Gaussian planetary equations, which showed to be more efficient, the orbit evolves as shown below over 1000 periods:

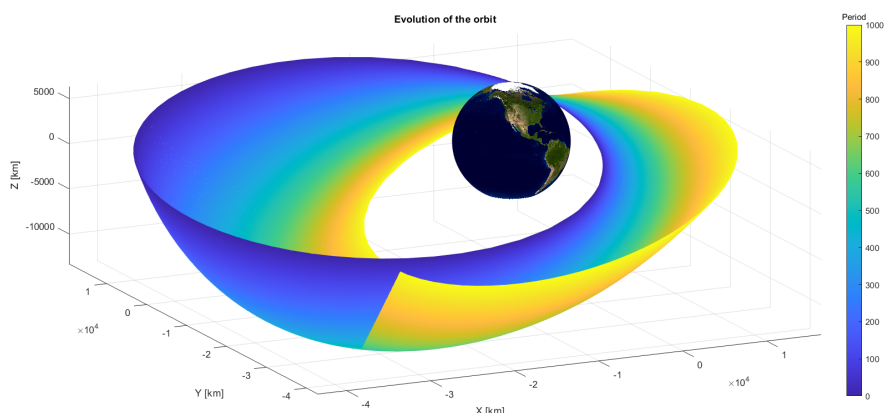


Figure 2.9: Propagation over 1000 orbits

2.6 Comparison with real data

The final goal was to compare the propagation method with real data from ephemerides. Of course, the propagator solution will not perfectly fit real data, since have been taken into account only the J_2 and the Moon perturbing effects, neglecting other sources of perturbations, such as the atmospheric drag, the solar radiation pressure and higher orders of the zonal harmonic gravity model. Have been selected the ephemerides of an Atlas 5 Centaur debris from Space-Track [3], which had similar orbital parameters compared to the assigned orbit in the first part of the analysis, so has the same main source of perturbation. The data cover more than one year, from 22/10/2021 to 22/12/2022, with a 3-days gap between each parameter.

Here reported the initial data of the chosen debris:

$a[\text{km}]$	$e[-]$	$i[\text{deg}]$	$\Omega[\text{deg}]$	$\omega[\text{deg}]$	$\theta[\text{deg}]$
$2.8674 \cdot 10^4$	0.5114	21.2516	302.7124	238.9207	113.6089

Table 2.3: Initial Orbital Parameters of the Debris

Using these data as starting condition the following results have been obtained:

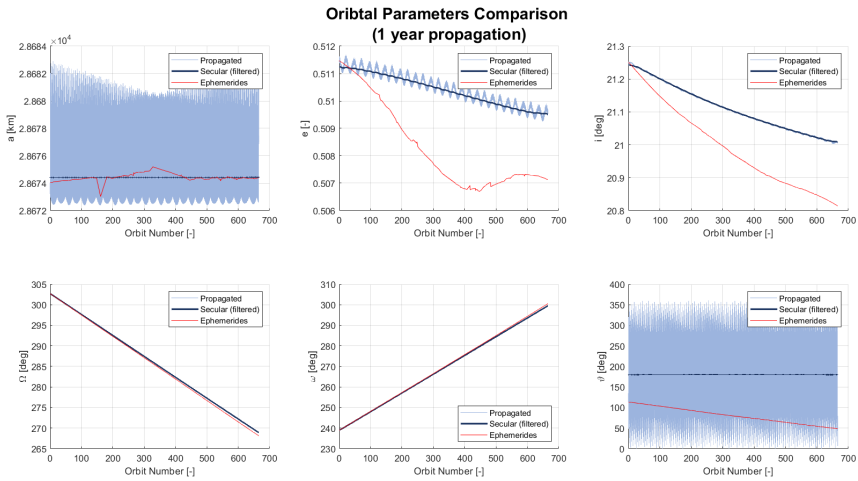


Figure 2.10: Comparison of keplerian elements with ephemerides over 1 year

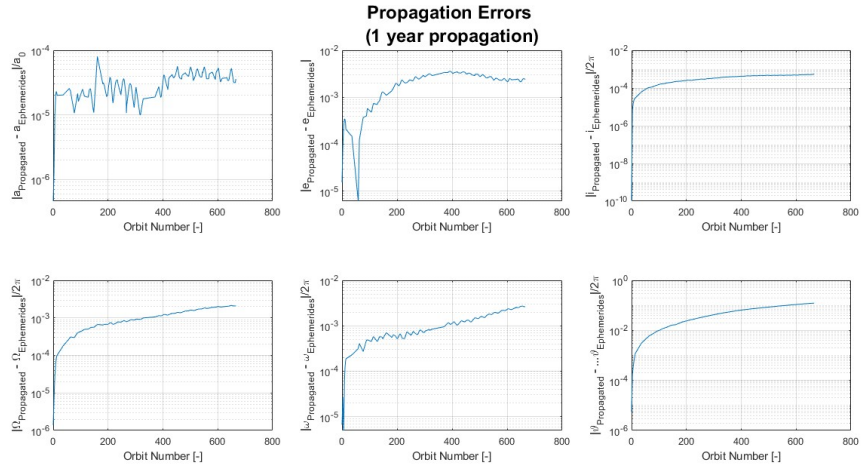


Figure 2.11: Difference between ephemerides and propagation from initial parameters

It can be noticed that there is a good correlation between the elements from the different methods, with error levels which are quite satisfying after more than a year of propagation time. The only value which has a secular trend different from the ephemerides is true anomaly. This last discrepancy is however not due to inaccuracies in the propagation method, but to the fact that the sampling frequency of the acquired data is too

low: the gap of 3 days for each measure is in fact very close to a multiple of the orbital period itself causing a phenomenon similar to aliasing.

Bibliography

- [1] Camilla Colombo. Course notes - orbital mechanics.
- [2] NASA. Saturn fact sheet. (visited: 22-12-2022).
- [3] Space-Track. Debris database. (visited: 22-12-2022).